Cell Death and Differentiation (2007) 14, 1095–1105

www.nature.com/cdd

# Insulin-like growth factor signaling regulates zebrafish embryonic growth and development by promoting cell survival and cell cycle progression

PJ Schlueter[1], G Peng[2], M Westerfield[2] and C Duan*[,1]

**Although much is known about the global effects of insulin-like growth factor 1 receptor (IGF1R)-mediated signaling on fetal growth and the clinical manifestations resulting from IGF/IGF1R deficiencies, we have an incomplete understanding of the cellular actions of this essential pathway during vertebrate embryogenesis. In this study, we inhibited IGF1R signaling during zebrafish embryogenesis using antisense morpholino oligonucleotides or a dominant-negative IGF1R fusion protein. IGF1R inhibition resulted in reduced embryonic growth, arrested development and increased lethality. IGF1R-deficient embryos had significant defects in the retina, inner ear, motoneurons and heart. No patterning abnormalities, however, were found in the brain or other embryonic tissues. At the cellular level, IGF1R inhibition increased caspase 3 activity and induced neuronal apoptosis. Coinjection of antiapoptotic *bcl2-like* mRNA attenuated the elevated apoptosis and rescued the retinal and motoneuron defects, but not the developmental arrest. Subsequent cell cycle analysis indicated an increased percentage of cells in G1 and a decreased percentage in S phase in IGF1R-deficient embryos independent of apoptosis. These results provide novel insight into the cellular basis of IGF1R function and show that IGF1R signaling does not function as an anteriorizing signal but regulates embryonic growth and development by promoting cell survival and cell cycle progression.**
*Cell Death and Differentiation* (2007) **14,** 1095–1105. doi:10.1038/sj.cdd.4402109; published online 2 March 2007

The insulin-like growth factor (IGF) signaling pathway is an evolutionarily conserved signaling cascade that is essential for proper vertebrate growth and development.[1–3] Activation of this critical pathway occurs when IGF ligands (IGF-1 and IGF-2) bind their cognate receptor tyrosine kinase, the IGF1 receptor (IGF1R). This leads to downstream activation of a number of signaling cascades, including mitogen-activated protein kinase and phosphatidylinositol 3-kinase.[4] *In vitro* studies using a variety of mammalian cell lines, primary cultured cells and tissue explants have demonstrated that IGF1R signaling stimulates cell proliferation and protects cells from a variety of apoptotic stimuli. The mitogenic and antiapoptotic actions of IGF1R signaling are further underscored by the resistance of IGF1R-/- fibroblasts to malignant transformation.[5]

Clinical studies have shown that human patients with loss-of-function mutations in either *IGF-1* or the *IGF1R* suffer severe intrauterine growth restriction and poor postnatal growth, as well as microcephaly, deafness and mental retardation.[6–10] Mouse genetic studies further established the causational importance of IGF1R signaling in fetal growth and development. *IGF1R* null mutant mice exhibited severe growth retardation at birth (45% of wild-type littermates) and died shortly after birth from respiratory failure. They also exhibited global organ hypoplasia and developmental retardation, with no loss of any organ or patterning abnormalities.[11,12] It has thus been concluded that IGF1R signaling is a central regulator of somatic growth in mammals.

Recent studies have shown that the major components of the IGF signaling pathway are conserved in lower vertebrates such as zebrafish.[3] It was reported that zebrafish have two distinct *igf1r* genes resulting from a gene duplication event at the *igf1r* locus and both are required for embryonic viability and proper growth and development.[13,14] Several studies in *Xenopus*, however, suggested that IGF1R signaling induces the formation of anterior neural tissue, the cellular basis for which was change in cell fate.[15,16] A similar study in zebrafish was also reported.[17] Thus, there is a major discrepancy concerning the cellular basis for the conserved IGF1R signaling cascade during vertebrate development.

In this study, we sought to investigate the developmental roles of IGF1R signaling during zebrafish embryogenesis and to elucidate the underlying cellular basis *in vivo*. We show that targeted knockdown or specific inhibition of IGF1R signaling resulted in reduced body size, retarded developmental rate and increased embryonic lethality. Despite the fact that IGF1R-deficient embryos had significant defects in the retina, inner ear, motoneurons and heart, no major patterning abnormalities were detected. We further provide evidence that the defects in retina and other neural tissues are primarily caused by elevated apoptosis, but the developmental arrest is

[1]Department of Molecular, Cellular and Developmental Biology, University of Michigan, Ann Arbor, MI, USA and [2]Institute of Neuroscience, University of Oregon, Eugene, OR, USA
*Corresponding author: C Duan, Department of Molecular, Cellular and Developmental Biology, University of Michigan, Ann Arbor, MI 48109, USA. Fax: 734 647 0884; E-mail: cduan@umich.edu
**Keywords:** insulin-like growth factor 1 receptor; embryogenesis; retina; heart; cell cycle; apoptosis
**Abbreviations:** Bcl2, B-cell lymphoma 2; CaP, caudal primary motoneuron; dnIGF1R:GFP, dominant-negative insulin-like growth factor 1 receptor:green fluorescent protein; IGF, insulin-like growth factor; IGF1R, insulin-like growth factor 1 receptor; IMO, morpholino oligonucleotide
Received 20.6.06; revised 28.11.06; accepted 21.12.06; Edited by E Baehrecke; published online 02.3.07

independent of apoptosis and correlates well with defects in cell cycle progression.

## Results

**Zebrafish *igf1r* knockdown causes growth retardation, developmental arrest and embryonic lethality but does not alter tissue patterning.** To elucidate the roles of IGF1R signaling during zebrafish embryogenesis, the *igf1r* genes (*igf1ra* and *igf1rb*) were knocked down with gene-specific MOs. Two distinct *igf1r* MOs were designed to target each *igf1r* gene. The efficacy and specificity of these *igf1r* MOs in targeting their receptors were recently confirmed.[13] In this study, we further verified the ability of these *igf1r* MOs to knockdown endogenous IGF1R proteins and inhibiting IGF1R signaling by biochemical analysis. As shown in Figure 1a, embryos injected with *igf1r* MOs have greatly reduced levels of total IGF1R protein compared to control MO-injected embryos. Further analysis showed a similar reduction in the levels of phosphorylated IGF1R (Figure 1b).

Previous work has shown that embryos with reduced IGF1R signaling exhibit significant reductions in both somite number and body length at 24 h postfertilization (hpf).[13] In this study, we examined *igf1r* MO-injected embryos at multiple time points during the first 24 h of development (Figure 1c). *Igf1r* MO-injected embryos developed normally until about 16 hpf. Their development slowed thereafter and arrested at approximately 18 hpf, whereas control MO-injected embryos continued to develop normally (Figure 1c). By 24 hpf, embryos

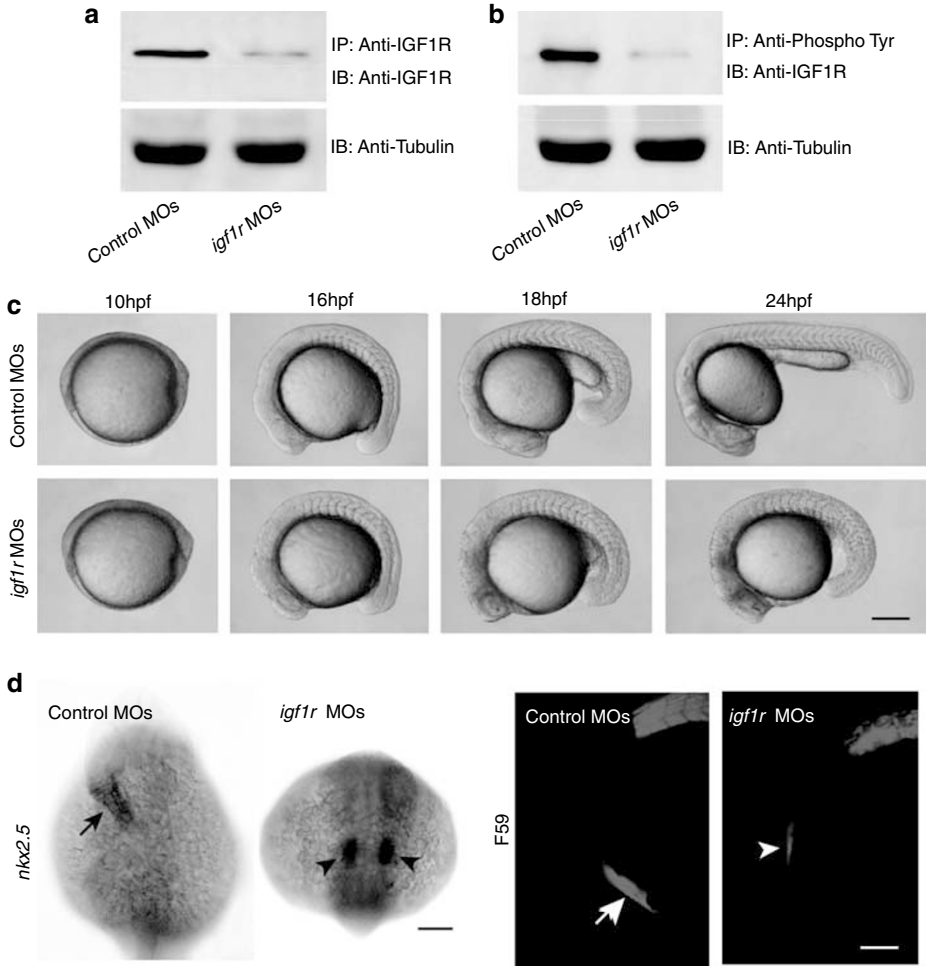


**Figure 1** IGF1R signaling is required for the proper growth, development and survival of zebrafish embryos. (**a**, **b**) The effect of *igf1r* MOs in knocking down IGF1R protein and inhibiting IGF1R signaling was analyzed at 24 hpf using IP followed by IB analysis. The antibodies used are indicated. An anti-Tubulin antibody was used to control for input and loading. Similar results were obtained in two other microinjection experiments. (**c**) Phenotypes of control (upper panels) and *igf1r* MO-injected embryos (lower panels) at 10, 16, 18 and 24 hpf. In three separate microinjection experiments, 78% of *igf1r* MO-injected embryos exhibited this phenotype ($N = 210$). Lateral views, anterior to the left. Scale bar = 250 μm. (**d**) Heart morphogenesis is retarded in *igf1r* MO-injected embryos compared to controls. Expression of *nkx2.5* mRNA in control and i*gf1r* MO-injected embryos at 24 hpf (left panels). Note the failure of the heart primordia in *igf1r* MO-injected embryos (black arrowheads) to fuse at the dorsal midline to form a heart tube, as in controls (black arrow). Dorsal views, anterior to the top. Scale bar = 100 μm. Similar patterns were observed in all 12–15 embryos examined in each group. F59 immunostaining in control and i*gf1r* MO-injected embryos at 24 hpf (right panels). Note the reduction in the cell mass and in ventral migration of the heart in *igf1r* MO-injected embryos (white arrowhead) compared to control MO-injected embryos (white arrow). Lateral views, anterior to the left, dorsal to the top. Scale bar = 100 μm. Similar patterns were observed in all embryos examined in each group ($N = 12$–15)

injected with *igf1r* MOs had only 16.5 + 2.1 somites compared to 29.8 ± 1.3 somites in the control group, indicating that they were developmentally equivalent to wild type or control embryos at 17–18 hpf. Additionally, *igf1r* MO-injected embryos lacked many anterior neuronal features, such as eyes and exhibited a lack of tissue transparency (Figure 1c). By 30 hpf (prim-15 stage), most *igf1r* MO-injected embryos died, whereas control MO-injected embryos were viable and morphologically indistinguishable from their wild-type siblings.

To investigate further this developmental arrest phenotype, we examined the timing of heart morphogenesis. *In situ* hybridization analysis of *nkx2.5* expression indicated that the heart primordia in *igf1r* MO-injected embryos failed to fuse at the dorsal midline even at 24 hpf (Figure 1d). This pattern resembled that of wild type or control embryos at 17–18 hpf.[18] Additionally, immunostaining with F59 for the ventricle-specific myosin heavy chain indicated that inhibition of IGF1R signaling resulted in a decrease in ventricle tissue and reduced migration of the heart toward the ventral side of the embryo (Figure 1d).

We next analyzed *igf1r* MO-injected embryos for potential patterning defects. We found that reduced IGF1R signaling did not alter brain patterning, as indicated by the mRNA expression of *emx1* (labeling forebrain), *eng2a* (hindbrain), *egr2b* (third and fifth rhombomeres) and *pax2a* (optic stalk, mid-hindbrain boundary, hindbrain) (Figure 2a–h), although the spatial domains of these markers were somewhat reduced in *igf1r* MO-injected embryos. The expression domains of *myoD* and *myogenin* were also reduced compared to controls (Figure 2m–p). We also analyzed the expression of *rx1* in the eye and *claudin a* in the otic vesicle and found the extent of expression to be more markedly reduced (Figure 2i–l).

To confirm that these defects found in *igf1r* MO-injected embryos are indeed caused by the loss of Igf1rs, MO-resistant mRNAs encoding full-length *igf1ra* and *igf1rb* were coinjected with *igf1r* MOs. As shown in Figure 3a, coinjection of the *igf1r* MOs along with *igf1ra* and *igf1rb* mRNA (*igf1r* mRNA) resulted in a significant recovery of normal growth and development. The mean body length increased from 47% of controls in *igf1r* MO-injected embryos to 80% in *igf1r* MOs ± *igf1r* mRNA-injected embryos. Somite number also increased from 16.7 ± 0.41 in *igf1r* MO-injected embryos to 23.9 ± 0.59 in *igf1r* MOs ± *igf1r* mRNA-injected embryos ($P < 0.0001$) (Figure 3c and d). Additionally, embryos with reduced IGF1R signaling exhibited a significant decrease in *rx1* expression in the retina, whereas embryos coinjected with *igf1r* MOs ± *igf1r* mRNA exhibited a substantial recovery of *rx1* expression (Figure 3b). Taken together, these data indicated that IGF1R signaling is required for proper zebrafish embryo growth and development but does not play an indispensable role in the patterning of brain or other embryonic tissues examined.

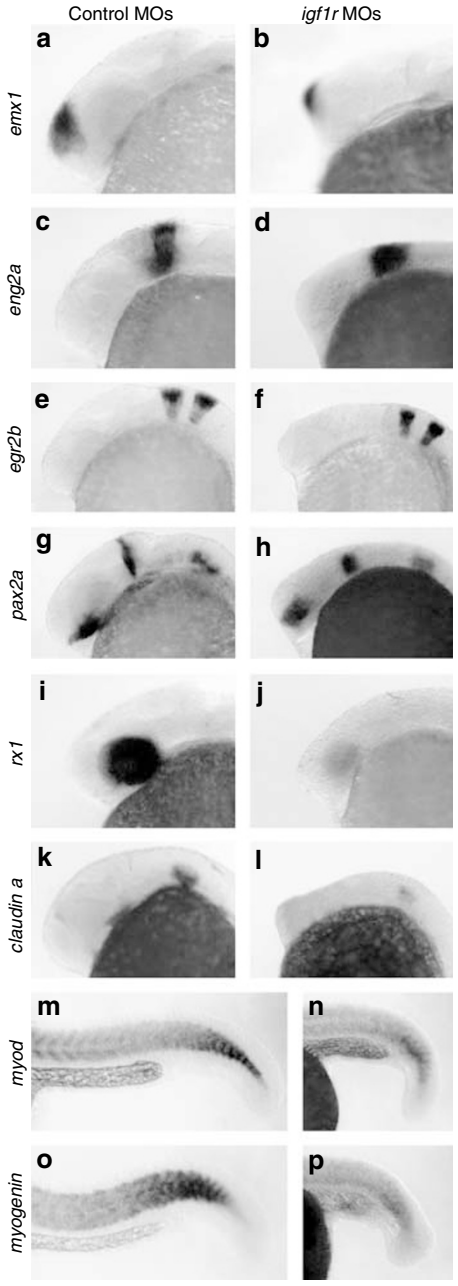


**Figure 2** Inhibition of IGF1R signaling does not alter embryo patterning. (**a**–**p**) Whole mount *in situ* hybridization analysis of various marker genes in control (left panels) and *igf1r* MO-injected (right panels) embryos at 24 hpf: *emx1* expression in the forebrain (**a**, **b**); *eng2*a expression in the mid-hindbrain boundary (**c**, **d**); *egr2b* expression in the third and fifth rhombomeres of the hindbrain (**e**, **f**); *pax2a* expression in the optic stalk, mid-hindbrain boundary and hindbrain (**g**, **h**); *rx1* expression in the retina (**i**, **j**); *claudin a* expression in the otic vesicle (**k**, **l**); *myoD* (**m**, **n**) and *myogenin* (**o**, **p**) expression in the somatic myotome. Similar patterns were observed in all embryos examined in each group ($N = 8$–10)

**Inhibition of IGF1R signaling results in increased neuronal apoptosis.** IGF1R signaling is a potent promoter of cell survival in a variety of cultured mammalian cells.[19–21] To test whether loss of IGF1R signaling leads to increased apoptosis in a developing vertebrate embryo, we measured the activity of caspase 3, an executioner caspase. Reducing IGF1R signaling resulted in a four-fold, highly significant increase in caspase 3 activities over controls and coinjection of the *igf1r* MOs along with *igf1r* mRNA reduced caspase 3 activities to the basal level (Figure 4a). We next performed TUNEL on cryosections of 20 hpf control and *igf1r* MO-injected embryos to decipher patterns of apoptosis. *Igf1r* MO-injected embryos had significantly greater numbers of

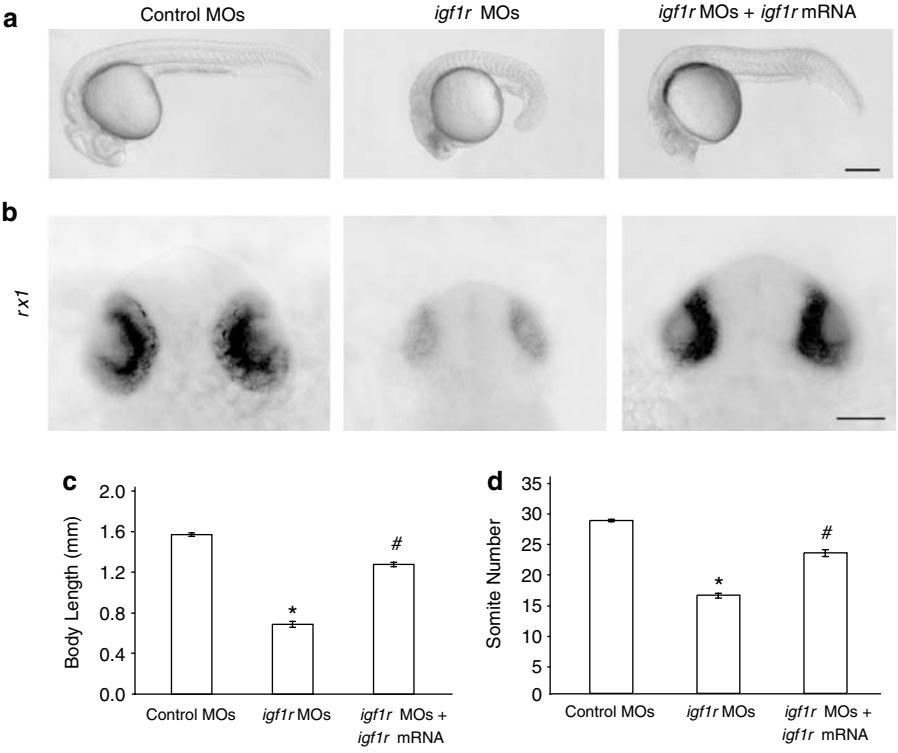


**Figure 3** Coinjection of *igf1r* mRNA with *igf1r* MOs rescues the growth and developmental defects. (**a**) Phenotypes of embryos injected with control MOs, *igf1r* MOs or *igf1r* MOs + *igf1r* mRNA at 24 hpf. In three separate microinjection experiments, 70% of *igf1r* MOs + *igf1r* mRNA-injected embryos exhibited this phenotype ($N = 252$). Lateral views, anterior to the left, dorsal to the top. Scale bar = 250 μm. (**b**) Expression of *rx1* mRNA in the retina of embryos injected with control MOs, *igf1r* MOs or *igf1r* MOs + *igf1r* mRNA at 24 hpf. Note the recovery of *rx1* expression upon coinjection of *igf1r* MOs with *igf1r* mRNA. Dorsal views, anterior to the top. Scale bar = 100 μm. Similar patterns were observed in all embryos examined in each group ($N = 12$–14). (**c**, **d**) Body length and somite number in embryos in the above treatment groups at 24 hpf. Graphs represent mean values of a total of 45 embryos resulting from three independent microinjection experiments. * $P < 0.0001$ between control and *igf1r* MO-injected embryos. # $P < 0.0001$ between *igf1r* MOs and *igf1r* MOs + *igf1r* mRNA-injected embryos

apoptotic cells throughout the brain region (Figure 4b). Concurrently, there was a substantial reduction in *rx1* mRNA expression in retinal tissues in *igf1r* MO-injected embryos (Figure 4c). TUNEL analysis of the trunk regions of these embryos revealed a similar increase in apoptosis in *igf1r* MO-injected embryos. The majority of apoptotic cells were found in the spinal cord (Figure 4d). The elevated neuronal apoptosis was reduced by coinjection of the *igf1r* MOs with *igf1r* mRNA (data not shown). Analysis of caudal primary motoneuron (CaP) by SV2 immunostaining indicated a reduction in the number of CaP motoneurons in *igf1r* MO-injected embryos (Figure 4e). These results strongly suggest that IGF1R signaling is an important survival signal for neuronal cells in developing zebrafish embryos.

To test whether this increased neuronal apoptosis was the cellular basis underlying the retina and CaP motoneuron defects in *igf1r* MO-injected embryos, zebrafish antiapoptotic *bcl2-like* (*bcl2l*) mRNA was coinjected with *igf1r* MOs to inhibit apoptosis. Injection of *bcl2l* mRNA caused a significant reduction of caspase 3 activity, greatly attenuated the increased apoptosis in the brain and spinal cord and resulted in a recovery of retina and CaP motoneurons (Figure 4a–e). These findings suggest that promotion of neuronal cell survival is a major mechanism by which IGF1R signaling regulates zebrafish retina and other neural tissue development.

**Expression of a dominant-negative IGF1R phenocopies igf1r MO-injected embryos.** The finding that IGF1R-deficient embryos progressed normally through development until approximately 16 hpf and then arrested at 18 hpf is both intriguing and puzzling, because both IGF ligands and IGF1Rs are expressed in a widespread fashion throughout all stages of embryogenesis.[14] Because it is known that maternal proteins can influence early development in zebrafish,[22] we postulated that maternal IGF1R protein may keep normal development up to 16 hpf. To test this idea and to investigate the developmental roles of IGF1R signaling further using an independent approach, a zebrafish dominant-negative IGF1R was constructed by deleting the intracellular signaling domain of IGF1Ra and tagging its C terminus with EGFP (dnIGF1R:GFP) (Figure 5a). Successful expression of the dnIGF1R:GFP fusion protein was confirmed by Western immunoblot (IB) using a GFP antibody (Figure 5b) and by observing GFP fluorescence microscopically (data not shown). Subsequent biochemical analysis revealed that overexpression of the dnIGF1R:GFP fusion protein did not alter total IGF1R protein levels but significantly diminished the levels of phosphorylated and activated IGF1Rs (Figure 5c). Further analysis revealed a major decrease in the levels of phosphorylated Akt (Figure 5d), which is a major downstream effector of the IGF1R.[4]

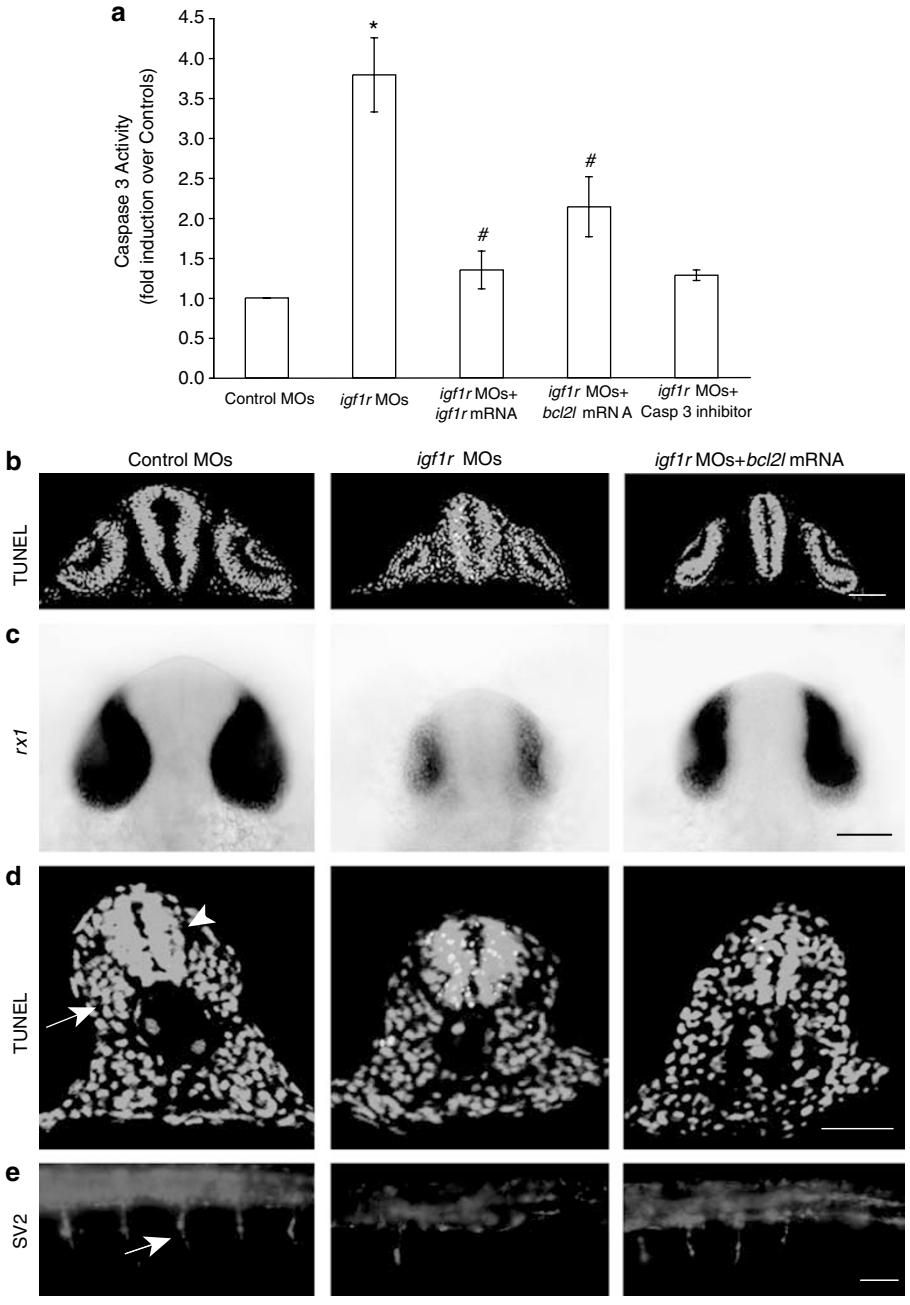


**Figure 4** Inhibition of IGF1R signaling increases neuronal apoptosis. (**a**) Caspase 3 activity in embryos injected with control MOs, *igf1r* MOs, *igf1r* MOs + *igf1r* mRNA and *igf1r* MOs + *bcl2l* mRNA at 24 hpf. The addition of a caspase 3 inhibitor, DEVD-fmk, to the lysates of *igf1r* MO-injected embryos was used as a control for specificity. The graph represents means from three independent microinjection experiments, each with 25 embryos per group. *$P<0.001$ for comparisons between control and *igf1r* MO-injected embryos. #, $P<0.001$ for comparisons between *igf1r* MO-injected embryos with either *igf1r* MOs + *igf1r* mRNA, or *igf1r* MOs + *bcl2l* mRNA-injected embryos. (**b**) TUNEL (red) of cryosections of brain regions from 20 hpf control MOs, *igf1r* MOs and *igf1r* MOs + *bcl2* mRNA-injected embryos. Nuclei were counterstained with sytox (green). Cross-sectional views, anterior to the top. Scale bar = 50 μm. (**c**) *Rx1* mRNA expression in control MOs, *igf1r* MOs and *igf1r* MOs + *bcl2* mRNA-injected embryos. Dorsal views, anterior to the top. Scale bar = 100 μm. (**d**) TUNEL (red) of cryosections of posterior trunk region of 20 hpf control MOs, *igf1r* MOs and *igf1r* MOs + *bcl2* mRNA-injected embryos. Nuclei were counterstained with sytox (green). The spinal cord (white arrowhead) and myotome (white arrow) are indicated in the control MO-injected embryo. Cross-sectional views, dorsal to the top. Scale bar = 20 μm. (**e**) SV2 labeling of CaP motoneurons in 20 hpf control MOs (white arrow), *igf1r* MOs and *igf1r* MOs + *bcl2* mRNA-injected embryos. Lateral views, anterior to the left, dorsal to the top. Scale bar = 100 μm. Similar patterns were observed in all embryos examined ($N = 12–15$)

Overexpression of the dnIGF1R:GFP fusion protein produced a growth-retarded and developmentally arrested embryo, similar to the phenotype of *igf1r* MO-injected embryos (Figure 5e). The mean somite number of *dnIGF1R:GFP* mRNA-injected embryos at 24 hpf (17.51 ± 1.24 somites) was significantly lower compared to control GFP mRNA-injected embryos (29.27 ± 0.78; $P<0.0001$). TUNEL analysis revealed a similar pattern of apoptosis as in *igf1r* MO-injected embryos, predominately in the brain and spinal cord (data not shown). In addition, caspase 3 activation was also

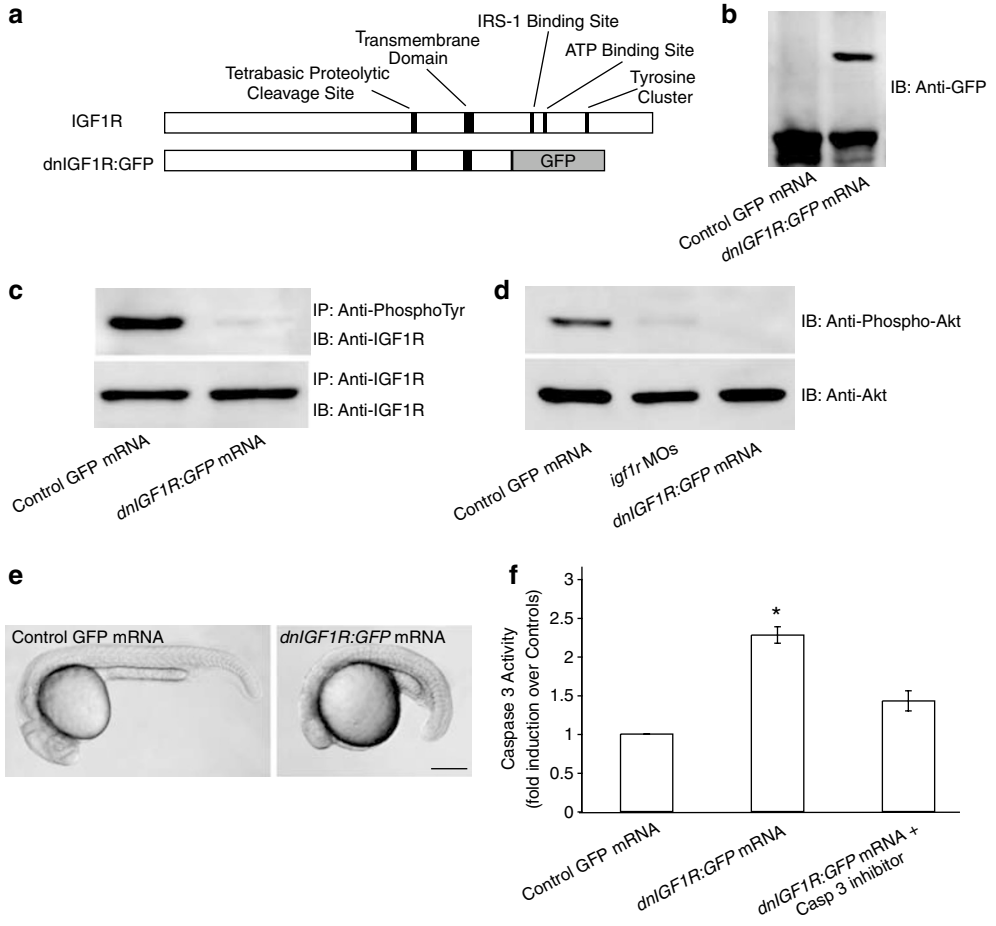


**Figure 5** Inhibition of IGF1R signaling by a dominant-negative IGF1R:GFP fusion protein (dnIGF1R:GFP). (**a**) A schematic diagram of the dnIGF1R:GFP fusion protein, which possesses transmembrane and dimerization domains but lacks the intracellular domain necessary for autophosphorylation and intracellular signaling. (**b**) Lysates from control GFP mRNA and *dnIGF1R:GFP* mRNA-injected embryos at 20 hpf were analyzed by IB using a GFP antibody. The dnIGF1R:GFP fusion protein was detected at the predicted ~60 kDa size, compared to the ~28 kDa band corresponding to GFP. (**c**) IP and IB analysis of 20 hpf embryos injected with either control GFP mRNA or *dnIGF1R:GFP* mRNA using IGF1R and phosphotyrosine antibodies. Similar results were obtained in two other microinjection experiments. (**d**) IB analysis of 20 hpf embryos injected with control GFP mRNA, *dnIGF1R:GFP* mRNA or *igf1r* MOs, using total and phospho-Akt antibodies. Similar results were obtained in two other microinjection experiments. (**e**) Phenotypes of control GFP mRNA and *dnIGF1R:GFP* mRNA-injected embryos at 24 hpf. In three separate microinjection experiments, 81% of *dnIGF1R:GFP* mRNA-injected embryos exhibited this phenotype ($N = 183$). (**f**) Caspase 3 activation in embryos injected with control GFP mRNA or *dnIGF1R:GFP* mRNA at 24 hpf. The graph represents mean values of three independent microinjection experiments, each with 25 embryos per group. The addition of a caspase 3 inhibitor, DEVD-fmk, to the lysates of *dnIGF1R:GFP* mRNA-injected embryos was used as a control for specificity. $^*P < 0.0001$ for comparisons between control GFP mRNA and *dnIGF1R:GFP* mRNA-injected embryos

significantly increased compared to control GFP mRNA-injected embryos (Figure 5f). These results indicated that expression of the dnIGF1R:GFP fusion protein effectively inhibited IGF1R signaling, and provide further evidence supporting a critical role for IGF1R signaling in promoting neuronal cell survival, as well as proper embryonic growth and development. They also suggest that the late onset of IGF1R loss-of-function phenotypes is not likely because of maternal IGF1R protein.

**Inhibition of IGF1R signaling does not alter early central nervous system patterning.** Given recent reports for a role for IGF signaling in the induction of anterior neural tissue and patterning[15–17], we tested whether *igf1r* MOs and *dnIGF1R:GFP* mRNA-injected embryos exhibited defects in patterning the central nervous system (CNS). Neither *igf1r* MOs nor *dnIGF1R:GFP* mRNA-injected embryos exhibited defects in CNS patterning, as indicated by the expression of *otx2* (presumptive forebrain and midbrain), *pax6b* (eye field and forebrain) and *shh* (notochord) at 10 hpf. As shown in Figure 6a, the expression patterns of these genes, which are all critical for normal neural development, are indistinguishable among controls, *igf1r* MOs and *dnIGF1R:GFP* mRNA-injected embryos. We next performed flow cytometry analysis at 10 hpf. Representative cell cycle histograms are shown in Figure 6b, and there are no major differences among the treatment groups in terms of the percentages of cells in each cell cycle phase (Figure 6b), although both *igf1r* MOs and *dnIGF1R:GFP* mRNA-injected embryos exhibited a modest but statistically significant increase in the percentages of cells in the $G_1$ phase

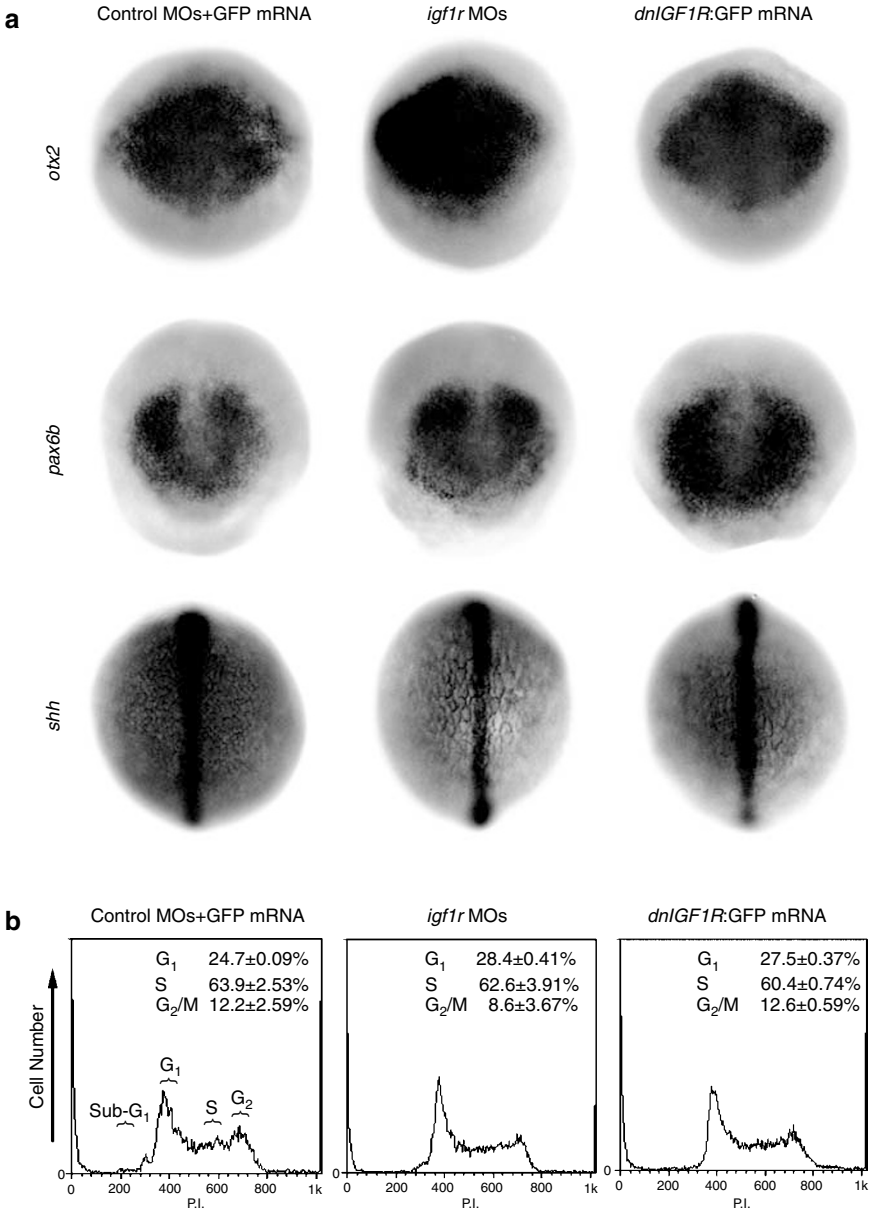


**Figure 6** Inhibition of IGF1R signaling does not alter CNS patterning. (**a**) Expression of *otx2* (presumptive forebrain and midbrain), *pax6b* (eye field and forebrain) and *shh* (notochord) is indistinguishable among controls, *igf1r* MO-injected embryos, and *dnIGF1R:GFP* mRNA-injected embryos at 10 hpf. Similar patterns were observed in all embryos examined in each group ($N = 12$–15). (**b**) Representative cell cycle histograms of control, *igf1r* MO-injected and *dnIGF1R:GFP* mRNA-injected embryos at 10 hpf. The mean percentages of cells in each phase of the cell cycle for three separate microinjection experiments are given (upper right of each histogram)

compared to controls. *igf1r* MOs and *dnIGF1R:GFP* mRNA-injected embryos were not significantly different from each other. Additionally, there were no significant sub-G1 peaks in control or IGF1R loss-of-function embryos, indicating low levels of apoptosis among all groups at this stage (Figure 6b).

**Inhibition of IGF1R signaling affects cell cycle progression.** Although overexpression of *bcl2l* in *igf1r* MO-injected embryos reduced apoptosis and rescued the retinal and motoneuron defects, it had no effect on the developmental arrest. As shown in Figure 7a, 24 hpf *igf1r* MOs $\pm$ *bcl2l* mRNA-injected embryos did not advance further than 18 hpf (18.13 $\pm$ 0.98 somites). We, therefore, tested whether the developmental arrest observed in *igf1r* MO-injected embryos was because of defects in cell proliferation. Indeed, *igf1r* MOs and *igf1r* MOs $\pm$ *bcl2l* mRNA-injected embryos exhibited significantly less BrdU-positive cells compared to controls (61 and 50% of the control group, respectively) (Figure 7b). To examine this cell proliferation defect in more detail, flow cytometry analysis was performed. Representative cell cycle histograms of 20 hpf embryos injected with control MOs, *igf1r* MOs, *igf1r* MOs $\pm$ *bcl2l* mRNA, or *igf1r* MOs $\pm$ *igf1r* mRNA are shown in Figure 7c. There is a clear increase in the amount of sub-$G_1$ cells in *igf1r* MO-injected embryos. Coinjection of *bcl2l* mRNA or

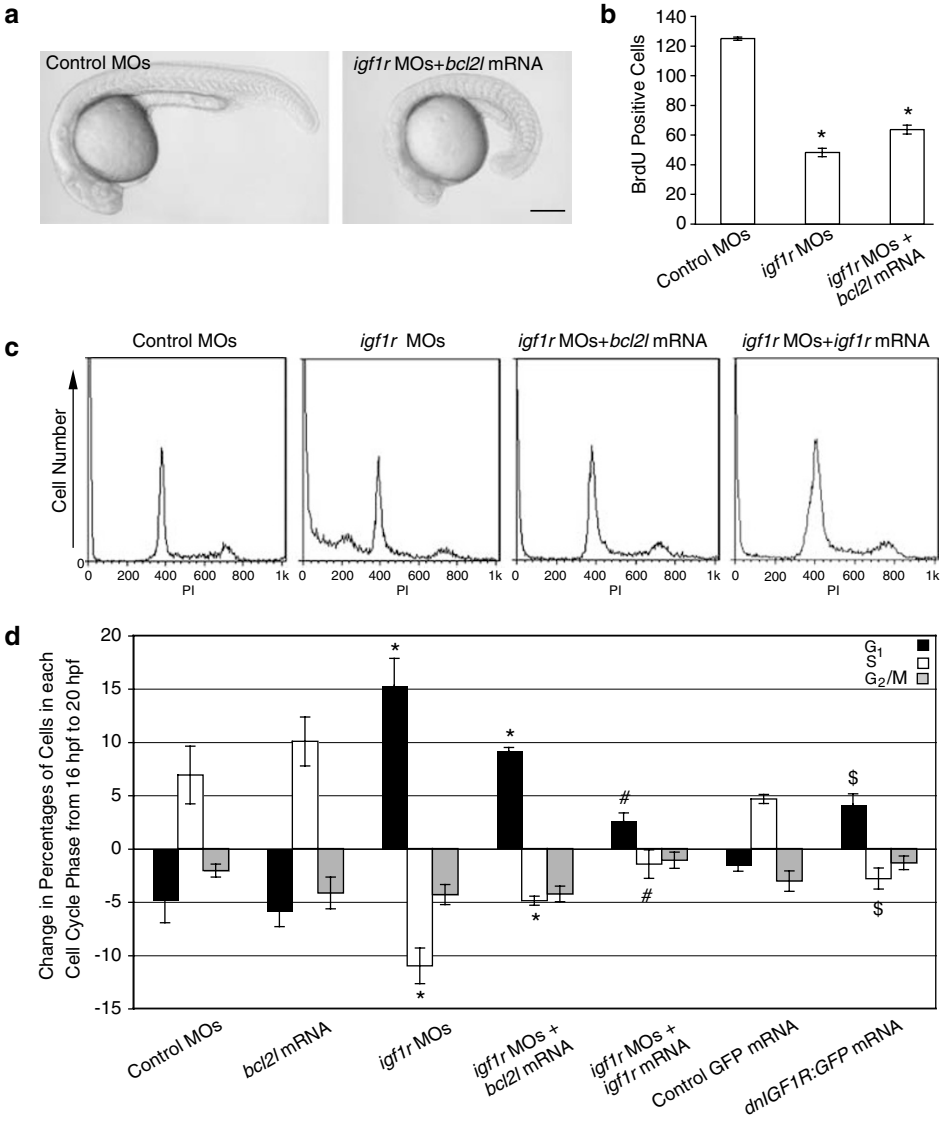


**Figure 7** Inhibition of IGF1R signaling causes cell cycle defects. (**a**) Phenotypes of embryos injected with either control MOs or *igf1r* MOs ± *bcl2l* mRNA at 24 hpf. In three separate microinjection experiments, 73% of *igf1r* MOs ± *bcl2l* mRNA-injected embryos exhibited this phenotype ($N = 176$). Scale bar = 250 μm. (**b**) Quantification of BrdU positive cells in 20 hpf embryos injected with control MOs, *igf1r* MOs or *igf1r* MOs ± *bcl2l* mRNA. Graph represents mean values of six embryos (from two independent microinjection experiments, each with 3 embryos per treatment group). *$P < 0.0001$ between control and *igf1r* MO-injected embryos, and between control and *igf1r* MOs ± *bcl2l* mRNA-injected embryos. (**c**) Representative cell cycle histograms of 20 hpf embryos injected with control MOs, *igf1r* MOs, *igf1r* MOs ± *bcl2l* mRNA or *igf1r* MOs ± *igf1r* mRNA. Note the reduction of the sub-$G_1$ peak in *igf1r* MO-injected embryos upon coinjection of either *bcl2l* mRNA or *igf1r* mRNA. (**d**) Changes in the percentages of cells in each cell cycle phase from 16 hpf to 20 hpf. Graph represents mean values of three independent microinjection experiments. *, $P < 0.0001$ for comparing the percentages of cells in the $G_1$ or S phase between control MO and *igf1r* MO-injected embryos, with or without coinjection of *bcl2l* mRNA. #, $P < 0.0002$ for comparing the percentages of cells in the $G_1$ or S phase between *igf1r* MOs and *igf1r* MOs ± *igf1r* mRNA-injected embryos. $, $P < 0.005$ for comparing the percentages of cells in the $G_1$ or S phase between control GFP mRNA and *dnIGF1R:GFP* mRNA-injected embryos

*igf1r* mRNA reduced it to control levels (Figure 7c), suggesting apoptotic inhibition.

When the change in the percentages of cells in each cell cycle phase, from 16 hpf (the onset of developmental arrest) to 20 hpf (2 h after developmental arrest), was quantified and compared, we found no significant differences in the cell cycle profiles between control MO and *bcl2l* mRNA-injected groups (Figure 7d). Both exhibited a decrease in the percentage of $G_1$-phase cells and an increase in the percentage of S-phase cells from 16 to 20 hpf. In contrast, *igf1r* MO-injected embryos exhibited a significant increase in the percentage of $G_1$-phase cells and a decrease in the percentage of S-phase cells from 16 to 20 hpf (Figure 7d). This significant increase in $G_1$-phase cells and decrease in S-phase cells suggests a defect in cell cycle progression at the $G_1$ to S transition in these *igf1r* MO-injected embryos and correlates well with the onset of developmental arrest. Apoptotic inhibition by coinjection of *bcl2l* mRNA did not alter these patterns (Figure 7d). Coinjection of *igf1r* mRNA partially, but significantly, restored normal cell cycle progression by decreasing the percentage of $G_1$-phase cells and increasing the percentage of S-phase cells (Figure 7d). Embryos injected with *dnIGF1F:GFP* mRNA

exhibited a significant increase in the percentage of $G_1$-phase cells and a significant decrease in the percentage of S-phase cells from 16 hpf to 20 hpf, compared to control GFP mRNA-injected embryos (Figure 7d). Together, these data suggested that the developmental arrest resulting from the inhibition of IGF1R signaling is independent of apoptosis but is correlated with a defect in the ability of embryonic cells to progress through the cell cycle.

## Discussion

Our loss-of-function study demonstrated that Igf1r-mediated signaling is required for the proper growth, development and survival of zebrafish embryos. Knockdown of the *igf1r* genes or specific inhibition of Igf1r-mediated signaling results in increased embryonic lethality. Igf1r-deficient embryos are significantly smaller in body length and they did not advance beyond a developmental stage equivalent to approximately 18 hpf in wild-type zebrafish but exhibited no patterning defects. These phenotypes are consistent with those reported in mutant mice[11,12,23] and *Drosophila*[24] but differ from previous studies in *Xenopus*.[15,16]

Although IGF signaling was proposed to be an anteriorizing or neural induction signal in *Xenopus*,[15,16] our results show that reduction of Igf signaling not only affects retina, but also other tissues throughout the zebrafish embryo. This is most evident in disrupted CaP motoneuron survival and increased apoptosis in the spinal cord. Depletion of Igf1r-mediated signaling also significantly delays heart morphogenesis and somitogenesis. These results indicate that Igf signaling exerts actions on most, if not all, embryonic tissues, and therefore does not function specifically as an anteriorizing signal in zebrafish. This conclusion is in good agreement with the widespread expression patterns of the Igf ligands and receptors in zebrafish embryos.[14] Differences in anterior neural induction between *Xenopus* and other vertebrates have been documented previously. For example, inhibiting BMP signaling by overexpressing follistatin, Noggin, or Chordin, anteriorizes *Xenopus* embryos;[25] however, BMP inhibition is not sufficient to induce a neural cell fate in chick or mouse embryos.[26] Similarly, overexpression of *cerberus* induces head formation in *Xenopus* embryos, but head formation is normal in mice null for *Cer1*.[27] There are also notable differences in the methodologies between our study and previous studies in *Xenopus* and zebrafish. In the current study, we employed two independent approaches to inhibit IGF1R signaling: multiple gene-specific MOs targeting both *igf1r* genes and a dominant-negative IGF1R fusion protein possessing the transmembrane domain. Both methods were shown to reduce IGF1R signaling *in vivo* effectively and they yielded similar phenotypes. The study by Richard-Parpaillon *et al*.[16] used only one *igf1r* MO targeting one *Xenopus igf1r* gene. Pera *et al*.[15] and Eivers *et al*.[17] overexpressed a secreted form of a truncated IGF1R lacking both the transmembrane and intracellular domains. The lack of a transmembrane anchor may affect its effectiveness as a dominant-negative inhibitor because there are a family of secreted IGF-binding proteins (insulin-like growth factor binding proteins), which bind IGFs with equal or even greater affinity than the IGF1R.[3,28–30] IGFBPs are present at high levels in specific embryonic tissues and could potentially outcompete a dominant-negative IGF1R that does not contain an appropriate membrane anchor, thereby reducing the knockdown efficacy in those tissues.

The easily accessible and transparent zebrafish embryo and the functional conservation of the IGF signaling system have provided an excellent opportunity for an in-depth investigation into the cellular basis of IGF signaling during early embryogenesis. Taking advantage of this model organism, we showed that knockdown or inhibition of the zebrafish IGF1R signaling significantly increased caspase 3 activity and TUNEL-positive cells. In the brains of IGF1R-deficient embryos, we observed a widespread pattern of apoptosis. In the trunk, apoptotic cells were concentrated in the spinal cord. Consistent with this increase in neuronal apoptosis, IGF1R-deficient embryos had a disproportionate reduction in retinal tissue compared to other anterior tissue and disruptions in CaP motoneuron formation/survival. Overexpression of *bcl2l* in IGF1R-deficient embryos led to a recovery of these tissues, strongly suggesting that IGF1R signaling regulates the development of the retina and CaP motoneurons, and possibly other neuronal tissues, by promoting cell survival.

It is interesting that embryos with reduced IGF1R signaling progressed normally until approximately 16 hpf and became arrested at $\sim$18 hpf. Reduced somite number and retarded heart morphogenesis was manifestations of this developmental arrest. In agreement with our findings in zebrafish, *igf1r* null mutant mice exhibit no significant differences in growth rate compared to wild-type littermates until embryonic day 11.0.[11,12] Whether elevated apoptosis played any role in these defects in developmental timing was not investigated. In this study, we found that overexpression of *bcl2l* could not restore normal developmental timing, suggesting that elevated apoptosis is unlikely the cellular basis underlying the developmental arrest. We noted that embryos with reduced IGF1R signaling exhibited a significant decrease in the number of proliferative cells, supporting the notion that endogenous IGF signaling may be required for embryonic cell cycle progression. Indeed, we found a significant increase in the percentage of $G_1$-phase cells and a significant decrease in the percentage of S-phase cells in embryos deficient in IGF1R signaling compared to controls. This phenotype was unaffected by apoptotic inhibition but could be rescued by coinjection of *igf1r* mRNA. These data indicate a strong correlation between the developmental arrest phenotype and defects in cell cycle progression at the $G_1$ to S transition. This conclusion is consistent with a recent study in mouse suggesting a role for IGF1 in accelerating the cell cycle by decreasing the G1 phase and increasing cell cycle reentry in the embryonic cerebral cortex.[31] Moreover, several studies in *Drosophila* point to a critical role for insulin receptor/IGF1R signaling in controlling the duration of embryonic development, total body size and organ size by regulating the rates of cell growth and proliferation.[32,33]

We and others have previously shown that the zebrafish IGF ligands and IGF1Rs are highly expressed in almost all tissues and at all stages of embryogenesis.[14,17] In fact, IGF, IGF1R and IGFBP transcripts are detected even at the one-cell stage.[3,14] It is, therefore, intriguing that the developmental

arrest phenotype in IGF1R-deficient embryos did not occur until approximately 16 hpf. The reason for this is yet unclear; however, it cannot be attributed to maternal IGF1R protein, because *igf1r* MOs and *dnIGF1R:GFP* mRNA-injected embryos exhibited nearly identical developmental arrest phenotypes. Future studies are needed to determine whether other components of the IGF signaling cascade, downstream of the IGF1R, are involved in the interesting developmental regulation of IGF1R signaling during zebrafish embryogenesis.

## Materials and Methods

**Animals and reagents.** Adult wild-type zebrafish (*Danio rerio*) were maintained at 28°C on a 14 h:10 h (light:dark) cycle and fed twice daily. Embryos were generated from natural crosses. Fertilized eggs were raised in embryo medium at 28.5°C and staged by hours postfertilization or standard criteria.[34] All experiments were conducted in accordance with guidelines approved by the University Committee on the Use and Care of Animals, University of Michigan.

All chemicals and reagents were purchased from Fisher Scientific (Pittsburgh, PA, USA) unless otherwise noted. RNase-free DNase was purchased from Promega (Madison, WI, USA). Restriction endonucleases were purchased from New England BioLabs (Beverly, MA, USA). Oligonucleotide primers for PCR were purchased from Invitrogen Life Technologies, Inc. (Carlsbad, CA, USA). The polyclonal IGF1R antibody (C-20) was purchased from Santa Cruz Biotechnology (Santa Cruz, CA, USA); the anti-phosphotyrosine antibody (PY20) from BD Biosciences (Franklin Lakes, NJ, USA) and the Tubulin antibody from Sigma. The SV2 monoclonal antibody was purchased from the Developmental Studies Hybridoma Bank (University of Iowa). The anti-Akt and anti-Phospho-Akt antibodies (Ser473) were purchased from Cell Signaling (Danvers, MA, USA) and the anti-GFP antibody was purchased from Torrey Pines Biolabs (Houston, TX, USA). Dr. F Stockdale from Stanford University generously provided the F59 antibody.

**Morpholino knockdown.** Gene-specific morpholino-modified oligonucleotides (MO) were purchased from Gene Tools, LLC (Philomath, OR, USA). Stock MO solutions were diluted in Danieau buffer and injected into fertilized embryos (1 nl/embryo) at the one- or two-cell stage, as previously described.[13] To ensure efficient knockdown of the *igf1r* genes, two nonoverlapping MOs were designed to target the translational start site and a region slightly upstream of that in the 5′UTR of each *igf1r* subtype; the specificity and efficacy of each of these MO sequences have been confirmed using multiple approaches.[13]

**Cloning and capped mRNA synthesis.** cDNAs encoding full-length *igf1ra* and *igf1rb* were amplified by RT-PCR using *Pfu* DNA Polymerase (Stratagene, La Jolla, CA, USA) along with the following primers: *igf1ra* 5′-TTGGTACCGACCATGGGATCTGGAACAGCGAGG-3′ and 5′-ACGACCATGTAG ACAAAGGGA-3′, and *igf1rb* 5′-TTGGTACCGACCATGGGGTCTAGCAAACAGA GG-3′ and 5′-GTCTCGAGCAGCAAGCCGAAGACTGG-3′. The resulted cDNAs were then cloned into the pBluescript II SK+ vector. To generate a dominant-negative *igf1ra* construct, a DNA fragment was amplified by RT-PCR using the following primers: 5′-TTGGTACCGACCATGGGATCTGGAACAGCGAGG-3′ and 5′-GTGGGCCCGCACAATGATGACAGCTACGAT-3′. This DNA fragment encodes a truncated IGF1Ra protein (from amino acids 1–974), containing the transmembrane and dimerization domains but lacks the tyrosine cluster, ATP binding site and the IRS-1 binding site. The same truncation in the human IGF1R has been shown to have the ability to form heterotetramers and the inability to activate intracellular signal transduction.[35] The amplified *igf1ra* PCR product was digested with *Apa*I and *Kpn*I and subcloned it into the *pHsp70*-GFP vector[36], thus creating a dominant-negative IGF1Ra:GFP fusion protein (dnIGF1R:GFP). This construct was then subcloned into pBluescript II SK+ using *Kpn*I and *Xho*I restriction sites, containing a previously inserted BGH polyA signal. A cDNA encoding the full-length zebrafish Bcl2-like (formerly known as BCL-xl) protein was cloned by RT-PCR based on sequences obtained from EST searches. The sequence is identical to a published cDNA sequence with the exception of one nucleotide in the 3′-UTR region.[37] The above constructs were linearized with *Not*I digests, and capped mRNAs encoding these proteins were synthesized using T7 polymerase, as previously reported.[38]

**Microinjection.** MO, plasmid DNA or mRNA solutions were injected into 1–2 cell embryos as reported previously.[38] To knockdown *igf1r* expression, we injected a mixture of all four MOs in the experiments described here. Each MO was injected at a final concentration of 1.25 ng/embryo, for a total of 5 ng MO/embryo. Two gene-specific missense control MOs were combined and injected at a final concentration of 2.5 ng/embryo for a total of 5 ng MO/embryo. For rescue experiments, *igf1ra* and *igf1rb* mRNA were coinjected (100 pg/embryo each) with *igf1r*a MO2 and *igf1rb* MO2 at 2.5 ng/embryo each. These mRNAs lack the 5′UTR and are resistant to the *igf1r* MOs targeting the 5′-UTR. The *dnIGF1Ra:GFP* mRNA was injected at a concentration of 750 pg/embryo. The *bcl2-like* mRNA was injected at a concentration of 200 pg/embryo. As a control for the *dnIGF1Ra:GFP* mRNA, we injected mRNA encoding GFP at a concentration of 750 pg/embryo.

**Body size and somite measurements.** Embryo body length was quantified by measuring the linear distance from the mid-hindbrain boundary to the tail, with a line parallel to the top (dorsal) and bottom (ventral) of the image**.** Each line was then measured using a scale taken at the same magnification. Somite number was quantified by counting total somite number per embryo.

**Immunoprecipitation and Western blot analysis.** About 20 embryos for each group were dechorionated, deyolked and homogenized in 200 μl of RIPA buffer (50 mM Tris-HCl, 150 mM NaCl, 2 mM EGTA, 0.1% Triton X-100, pH 7.5), containing 10 μg/ml aprotinin, 10 μg/ml leupeptin, 10 μg/ml pepstatin, 100 mM PMSF and 0.1 M sodium orthovanadate. The homogenates were briefly centrifuged to pellet cellular debris. Protein levels of each sample were quantified using a protein assay kit (Pierce Biotechnology Inc., Rockford, IL, USA). Equal amounts of protein were subjected to immunoprecipitation (IP) using either the phosphotyrosine antibody or the IGF1R antibody, or to Western blot analysis. For IP analysis, lysates were precleared using 15 μl Protein G Agarose beads (50% slurry) (Upstate Cell Signaling Solutions, Chicago, IL, USA). After the precleared lysate was transferred to a new tube, 5 μg antibody was added and rotated at 4°C for 2 h. Protein G Agarose beads (30 μl) were then added to the samples and rotated for another 2 h at 4°C, after which they were briefly centrifuged to pellet the beads. The supernatant was removed and stored for Western blot analysis. The beads were washed once with 1 × PBS, pelleted and then the supernatant was discarded. The beads were boiled for 5 min in protein sample buffer (250 mM Tris-HCl, pH 6.8, 5% SDS, 0.25% bromophenol blue, 25% glycerol) under reducing conditions. The beads were pelleted again and the supernatant was subjected to Western blot analysis, which was performed as described previously.[38] The anti-phosphotyrosine, Tubulin and GFP antibodies were used at 1 : 1000 dilution, and the anti-Phospho-Akt, total Akt and IGF1R antibodies were used at 1 : 500 dilution.

**Whole mount *in situ* hybridization and immunocytochemistry.** Whole mount *in situ* hybridization using digoxigenin (DIG)-labeled RNA riboprobes and whole mount immunocytochemistry was carried out as reported previously.[14] For immunocytochemistry, heart ventricle tissue was labeled with a 1 : 10 dilution of F59, and motoneuron axons were detected with a 1 : 2000 dilution of anti-SV2. A 1 : 100 dilution of a Cy3-conjugated secondary antibody (Jackson ImmunoResearch Laboratories, West Grove, PA, USA) was used to detect primary antibodies. Images were viewed using a Nikon DC50NN camera mounted to a Nikon Eclipse E600 microscope.

**Apoptosis assays.** Embryo embedding, freezing and sectioning protocols were performed according to Hu *et al.*[39] Sections (10 μm) were collected and air-dried at room temperature for 2 h before staining or storage at −20°C. For TUNEL assays, sections were stained using the In Situ Cell Death Detection Kit, TMR Red, according to the manufacturer's instructions (Roche, Nutlet, NJ, USA). Nuclei were counterstained with 50 nM sytox (Molecular Probes, Carlsbad, CA, USA). Images were captured using a Nikon DC50NN camera mounted to a Nikon Eclipse E600 microscope. Images of TUNEL and sytox staining were captured separately and then merged using Adobe Photoshop. Whole mount TUNEL staining was also performed according to the manufacturer's instructions, and images were also captured using a Nikon DC50NN camera mounted to a Nikon Eclipse E600 microscope.

Caspase 3 activity was measured using the ApoAlert caspase 3 Activation Assay Kit (BD Biosciences, Franklin Lakes, NJ, USA) according to the manufacturer's instructions. Final values are expressed as fold induction of caspase 3 activity over controls (control MO-injected embryos or control GFP mRNA-injected embryos).

**BrdU analysis.** Whole mount BrdU analysis of proliferative cells was done according to Gray *et al.*[40] Briefly, embryos were soaked in BrdU solution for 20 min, transferred to water lacking BrdU for 30 min, then fixed and stained with a 1 : 100 dilution of a BrdU antibody (Invitrogen, Carlsbad, CA, USA). A 1 : 500 dilution of a Cy3-conjugated secondary antibody (Jackson ImmunoResearch Laboratories, West Grove, PA, USA) was used to detect the primary antibodies. Embryos were analyzed and images were captured using laser scanning confocal microscopy (Model LSM 510, Carl Zeiss, Thornwood, NJ, USA). Thirty-five serial sections (5 $\mu$m) were taken off the brain of each embryo, including the area from the mid-hindbrain boundary forward to the forebrain. Fluorescent cells were counted in each section and care was taken to count each BrdU-positive cell only once, despite appearing in multiple sections.

**Flow cytometry analysis.** Cell cycle analysis was carried out using a FACSCalibur flow cytometer (BD Biosciences, Franklin Lakes, NJ, USA). Briefly, 40 deyolked embryos were homogenized in 1.5 ml of DMEM + 10% fetal calf serum (FCS). Single-cell suspensions were obtained by sequentially straining the homogenates through 105 $\mu$m and 40 $\mu$m mesh filters. The cells were then washed and fixed in ethanol. After fixation, a propidium iodide (PI) staining solution (50 $\mu$g/ml PI, 100 $\mu$g/ml RNAse Type I, 0.1% sodium citrate, 0.0002% Triton X-100) was added, and the cells were incubated for 1 h in the dark at 4°C. Samples were then subjected to flow cytometric analysis, using CellQuest Pro software (BD Biosciences, Franklin Lakes, NJ, USA). A two-parameter dot-plot of forward light scatter *versus* side scatter was constructed along with a two-parameter dot-plot of FL2 (PI) area *versus* width. In addition, a single-parameter PI (area) histogram was constructed to illustrate relative DNA content in each cell cycle phase. Cell cycle analysis (percentages of cells in each cell cycle phase) based on PI incorporation was done using Modfit LT (Verity Software House). Coefficients of variation were less than 5% in all experimental groups.

**Statistics.** Quantitative data are presented as means ± standard error (S.E.M.). Differences among groups were statistically compared using one-way ANOVA followed with Fisher's *post hoc* tests. Differences between groups were statistically compared using unpaired *t*-tests.

**Acknowledgements**. We thank Drs. D Goldman, M Ekker, F Stockdale, R Kollmar, S Lyons, P Raymond and SJ Du for kindly providing reagents for this work. This study was supported by NSF IBN 0110864 to CD.

1. LeRoith D. Insulin-like growth factor I receptor signaling—overlapping or redundant pathways? *Endocrinology* 2000; **141**: 1287–1288.
2. Nakae J, Kido Y, Accili D. Distinct and overlapping functions of insulin and IGF-I receptors. *Endocr Rev* 2001; **22**: 818–835.
3. Wood AW, Duan C, Bern HA. Insulin-like growth factor signaling in fish. *Int Rev Cytol* 2005; **243**: 215–285.
4. Dupont J, LeRoith D. Insulin and insulin-like growth factor I receptors: similarities and differences in signal transduction. *Horm Res* 2001; **55**: 22–26.
5. Valentinis B, Baserga R. IGF-I receptor signalling in transformation and differentiation. *Mol Pathol* 2001; **54**: 133–137.
6. Abuzzahab MJ, Schneider A, Goddard A, Grigorescu F, Lautier C, Keller E *et al.* IGF-I receptor mutations resulting in intrauterine and postnatal growth retardation. *N Engl J Med* 2003; **349**: 2211–2222.
7. Denley A, Wang CC, McNeil KA, Walenkamp MJ, Van Duyvenvoorde H, Wit JM *et al.* Structural and functional characteristics of the Val44Met insulin-like growth factor I missense mutation: correlation with effects on growth and development. *Mol Endocrinol* 2005; **19**: 711–721.
8. Kawashima Y, Kanzaki S, Yang F, Kinoshita T, Hanaki K, Nagaishi J *et al.* Mutation at cleavage site of insulin-like growth factor receptor in a short-stature child born with intrauterine growth retardation. *J Clin Endocrinol Metab* 2005; **90**: 4679–4687.
9. Walenkamp MJ, Karperien M, Pereira AM, Hilhorst-Hofstee Y, Van Doorn J, Chen JW *et al.* Homozygous and heterozygous expression of a novel insulin-like growth factor-I mutation. *J Clin Endocrinol Metab* 2005; **90**: 2855–2864.
10. Woods KA, Camacho-Hubner C, Savage MO, Clark AJ. Intrauterine growth retardation and postnatal growth failure associated with deletion of the insulin-like growth factor I gene. *N Engl J Med* 1996; **335**: 1363–1367.
11. Baker J, Liu JP, Robertson EJ, Efstratiadis A. Role of insulin-like growth factors in embryonic and postnatal growth. *Cell* 1993; **75**: 73–82.
12. Liu JP, Baker J, Perkins AS, Robertson EJ, Efstratiadis A. Mice carrying null mutations of the genes encoding insulin-like growth factor I (Igf-1) and type 1 IGF receptor (Igf1r). *Cell* 1993; **75**: 59–72.
13. Schlueter PJ, Royer T, Farah MH, Laser B, Chan SJ, Steiner DF *et al.* Gene duplication and functional divergence of the zebrafish insulin-like growth factor 1 receptors. *FASEB J* 2006; **20**: 1230–1232.
14. Maures T, Chan SJ, Xu B, Sun H, Ding J, Duan C. Structural, biochemical, and expression analysis of two distinct insulin-like growth factor I receptors and their ligands in zebrafish. *Endocrinology* 2002; **143**: 1858–1871.
15. Pera EM, Wessely O, Li SY, De Robertis EM. Neural and head induction by insulin-like growth factor signals. *Dev Cell* 2001; **1**: 655–665.
16. Richard-Parpaillon L, Heligon C, Chesnel F, Boujard D, Philpott A. The IGF pathway regulates head formation by inhibiting Wnt signaling in Xenopus. *Dev Biol* 2002; **244**: 407–417.
17. Eivers E, McCarthy K, Glynn C, Nolan CM, Byrnes L. Insulin-like growth factor (IGF) signalling is required for early dorso-anterior development of the zebrafish embryo. *Int J Dev Biol* 2004; **48**: 1131–1140.
18. Serbedzija GN, Chen JN, Fishman MC. Regulation in the heart field of zebrafish. *Development* 1998; **125**: 1095–1101.
19. Vincent AM, Feldman EL. Control of cell survival by IGF signaling pathways. *Growth Horm IGF Res* 2002; **12**: 193–197.
20. Peruzzi F, Prisco M, Dews M, Salomoni P, Grassilli E, Romano G *et al.* Multiple signaling pathways of the insulin-like growth factor 1 receptor in protection from apoptosis. *Mol Cell Biol* 1999; **19**: 7203–7215.
21. Resnicoff M, Abraham D, Yutanawiboonchai W, Rotman HL, Kajstura J, Rubin R *et al.* The insulin-like growth factor I receptor protects tumor cells from apoptosis *in vivo*. *Cancer Res* 1995; **55**: 2463–2469.
22. Pelegri F. Maternal factors in zebrafish development. *Dev Dyn* 2003; **228**: 535–554.
23. Wang ZQ, Fung MR, Barlow DP, Wagner EF. Regulation of embryonic growth and lysosomal targeting by the imprinted Igf2/Mpr gene. *Nature* 1994; **372**: 464–467.
24. Brogiolo W, Stocker H, Ikeya T, Rintelen F, Fernandez R, Hafen E. An evolutionarily conserved function of the Drosophila insulin receptor and insulin-like peptides in growth control. *Curr Biol* 2001; **11**: 213–221.
25. Dale L, Jones CM. BMP signalling in early Xenopus development. *Bioessays* 1999; **21**: 751–760.
26. Wilson SI, Edlund T. Neural induction: toward a unifying mechanism. *Nat Neurosci* 2001; **4** (Suppl): 1161–1168.
27. Belo JA, Bachiller D, Agius E, Kemp C, Borges AC, Marques S *et al.* Cerberus-like is a secreted BMP and nodal antagonist not essential for mouse development. *Genesis* 2000; **26**: 265–270.
28. Jones JI, Clemmons DR. Insulin-like growth factors and their binding proteins: biological actions. *Endocr Rev* 1995; **16**: 3–34.
29. Firth SM, Baxter RC. Cellular actions of the insulin-like growth factor binding proteins. *Endocr Rev* 2002; **23**: 824–854.
30. Hsieh T, Gordon RE, Clemmons DR, Busby Jr WH, Duan C. Regulation of vascular smooth muscle cell responses to insulin-like growth factor (IGF)-I by local IGF-binding proteins. *J Biol Chem* 2003; **278**: 42886–42892.
31. Hodge RD, D'Ercole AJ, O'Kusky JR. Insulin-like growth factor-I accelerates the cell cycle by decreasing G1 phase length and increases cell cycle reentry in the embryonic cerebral cortex. *J Neurosci* 2004; **24**: 10201–10210.
32. Chen C, Jack J, Garofalo RS. The Drosophila insulin receptor is required for normal growth. *Endocrinology* 1996; **137**: 846–856.
33. Shingleton AW, Das J, Vinicius L, Stern DL. The temporal requirements for insulin signaling during development in Drosophila. *PLoS Biol* 2005; **3**: e289.
34. Kimmel CB, Ballard WW, Kimmel SR, Ullmann B, Schilling TF. Stages of embryonic development of the zebrafish. *Dev Dyn* 1995; **203**: 253–310.
35. Prager D, Yamasaki H, Weber MM, Gebremedhin S, Melmed S. Human insulin-like growth factor I receptor function in pituitary cells is suppressed by a dominant-negative mutant. *J Clin Invest* 1992; **90**: 2117–2122.
36. Li Q, Shirabe K, Kuwada JY. Chemokine signaling regulates sensory cell migration in zebrafish. *Dev Biol* 2004; **269**: 123–136.
37. Chen MC, Gong HY, Cheng CY, Wang JP, Hong JR, Wu JL. Cloning and characterization of zfBLP1, a Bcl-XL homologue from the zebrafish, Danio rerio. *Biochim Biophys Acta* 2001; **1519**: 127–133.
38. Li Y, Xiang J, Duan C. Insulin-like growth factor binding protein-3 (IGFBP-3) plays an important role in regulating pharyngeal skeleton and inner ear formation and differentiation. *J Biol Chem* 2005; **280**: 3613–3620.
39. Hu M, Easter SS. Retinal neurogenesis: the formation of the initial central patch of postmitotic cells. *Dev Biol* 1999; **207**: 309–321.
40. Gray M, Moens CB, Amacher SL, Eisen JS, Beattie CE. Zebrafish deadly seven functions in neurogenesis. *Dev Biol* 2001; **237**: 306–323.